



HAL
open science

Derivation of a polynomial equation for the boundaries of 2-X manipulators

Matthieu Furet, Philippe Wenger

► **To cite this version:**

Matthieu Furet, Philippe Wenger. Derivation of a polynomial equation for the boundaries of 2-X manipulators. 2018. hal-01905469

HAL Id: hal-01905469

<https://hal.science/hal-01905469>

Preprint submitted on 6 Nov 2018

HAL is a multi-disciplinary open access archive for the deposit and dissemination of scientific research documents, whether they are published or not. The documents may come from teaching and research institutions in France or abroad, or from public or private research centers.

L'archive ouverte pluridisciplinaire **HAL**, est destinée au dépôt et à la diffusion de documents scientifiques de niveau recherche, publiés ou non, émanant des établissements d'enseignement et de recherche français ou étrangers, des laboratoires publics ou privés.

Derivation of a polynomial equation for the boundaries of 2-X manipulators

Matthieu Furet and Philippe Wenger

Laboratoire des Sciences du Numérique de Nantes (LS2N), CNRS, Ecole Centrale de Nantes, 44321 Nantes, France

Abstract. This paper derives the boundary equations of the workspace of a manipulator made of two crossed four-bar mechanisms in series. The boundaries are determined with the discriminant of the characteristic polynomial derived for the inverse kinematics.

Keywords: Kinematics, crossed four-bar mechanism, anti-parallelogram, Workspace, Cuspidal

1 Introduction

A crossed four-bar mechanism, referred to as X-mechanism, is a four-bar mechanism assembled in a X-shape configuration, see figure 1. Because of a variable instantaneous center of rotation (ICR), this mechanism has a large range of motion. Moreover, tendon driven actuation can be easily implemented and a lightweight manipulator with remote actuation can be designed by stacking several such mechanisms [1]. Eventually, lateral springs can be added on each side of the mechanism, thus defining a X-shape Snelson tensegrity mechanism [2], suitable for variable stiffness and natural interaction with the environment [3],[9]. This work is part of the AVINECK project involving biologists and roboticists with the main goal to model and design bird necks. Accordingly, a class of planar tensegrity manipulators made of a series assembly of several Snelson's X-shape mechanisms has been chosen as a suitable candidate for a preliminary planar model of a bird neck. A planar two-degree-of-freedom manipulator is obtained with a series assembly of two such mechanisms. First investigations on the kinematics of such manipulators have proven more challenging than expected, in particular for the solution of the inverse kinematics [10]. This paper derives the boundary equations of the workspace of a manipulator made of two crossed four-bar mechanisms in series. The boundaries are determined with the discriminant of the characteristic polynomial derived for the inverse kinematics. It is found that internal boundary curves may exist with cusp points [11], showing that the manipulator at hand is cuspidal ([15], [16]).

2 Manipulator modelling and Kinematic equations

The manipulators studied consist of a series assembly of two identical X-mechanisms as shown in figure 2. Both the base bar and the upper bar are of length

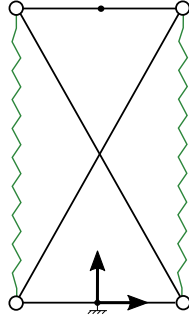


Fig. 1: Snelson's X-shape mechanism made of a crossed four-bar mechanism with lateral springs

b and the two crossed links are of length L with $L > b$. Thus, each X-mechanism defines a so-called anti-parallelgram joint. A line segment of length l_i is defined that links the middle points of the top and base bars of each mechanism i (shown in red dotted line in figure 2). The angle between this line and the direction orthogonal to the base bar, referred to as θ_i , is used to define the configuration of mechanism i without ambiguity, assuming that it remains always in its crossed-bar assembly mode [10]. Accordingly, the manipulator configuration can be fully defined with (θ_1, θ_2) . To avoid any self collisions, the bars should be assembled in different layers or suitable joint limits should be defined. The base frame is centered at the middle point of the base bar of the first X-mechanism with the x-axis aligned along this bar. The reference point (x, y) is chosen as the middle point of the top-bar of the second X-mechanism (figure 2). Since the sides of

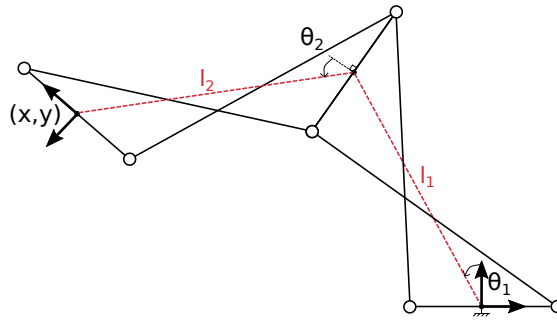


Fig. 2: Manipulator description

each mechanism define an isosceles trapezoid, the length l_i of the line segment that links the middle points of the top and base bars can be expressed as follows [10]:

$$l_i(\theta_i) = \sqrt{L^2 - b^2 \cos^2(\theta_i)} \quad (1)$$

The direct kinematic equations of the 2-X manipulator can be put in the following form :

$$\begin{cases} x = -l_1(\theta_1) \sin(\theta_1) - l_2(\theta_2) \sin(2\theta_1 + \theta_2) \\ y = l_1(\theta_1) \cos(\theta_1) + l_2(\theta_2) \cos(2\theta_1 + \theta_2) \end{cases} \quad (2)$$

where l_1 and l_2 are defined in (1). Note that these equations assume that each mechanism remains in its crossed-bar assembly-mode.

The inverse kinematics is much more challenging to establish and cannot be obtained from (2) easily. A methodology was proposed in [10], which makes it possible to derive a characteristic polynomial of degree four and it was shown that the manipulator may have up to four solutions.

3 Workspace boundary equations

The manipulator workspace is determined by means of its boundaries. These boundaries can be obtained from the discriminant of the 4th-order characteristic polynomial derived for the inverse kinematics. This characteristic polynomial in $t=\tan(\phi_1/2)$ was derived in [10] and is recalled below, where L has been set to 1 without loss of generality:

$$a_4 t^4 + a_3 t^3 + a_2 t^2 + a_1 t + a_0 = 0 \quad (3)$$

where :

$$a_4 = (b+1)^2(b^2 y^2 + x^4 + 2x^2 y^2 + y^4 + 4x^3 + 4x y^2 + 5x^2 + y^2 + 2x) \quad (4)$$

$$a_3 = 4y(b+1)(2b^2 x + b^2 - 2x^2 - 2y^2 - 4x - 1) \quad (5)$$

$$a_2 = 2(b^4 y^2 + b^2 x^4 + 2b^2 x^2 y^2 + b^2 y^4 + b^2 x^2 - 10b^2 y^2 + x^4 + 2x^2 y^2 + y^4 - 3x^2 + 9y^2) \quad (6)$$

$$a_1 = 4y(b-1)(2b^2 x - b^2 + 2x^2 + 2y^2 - 4x + 1) \quad (7)$$

$$a_0 = (b-1)^2(b^2 y^2 + x^4 + 2x^2 y^2 + y^4 - 4x^3 - 4x y^2 + 5x^2 + y^2 - 2x) \quad (8)$$

The discriminant of this polynomial is derived with the help of a symbolic computing software. Accordingly, a polynomial equation of degree 16 in x and y is obtained as shown below.

$$\begin{aligned} & 4b^{14}y^6 + 12b^{12}x^4y^4 + 28b^{12}x^2y^6 + 17b^{12}y^8 + 12b^{10}x^8y^2 + 60b^{10}x^6y^4 + 112b^{10}x^4y^6 + \\ & 92b^{10}x^2y^8 + 28b^{10}y^{10} + 4b^8x^{12} + 36b^8x^{10}y^2 + 126b^8x^8y^4 + 224b^8x^6y^6 + 216b^8x^4y^8 + \\ & 108b^8x^2y^{10} + 22b^8y^{12} + 4b^6x^{14} + 32b^6x^{12}y^2 + 108b^6x^{10}y^4 + 200b^6x^8y^6 + 220b^6x^6y^8 + \\ & 144b^6x^4y^{10} + 52b^6x^2y^{12} + 8b^6y^{14} + b^4x^{16} + 8b^4x^{14}y^2 + 28b^4x^{12}y^4 + 56b^4x^{10}y^6 + \\ & 70b^4x^8y^8 + 56b^4x^6y^{10} + 28b^4x^4y^{12} + 8b^4x^2y^{14} + b^4y^{16} - 24b^{12}x^2y^4 - 36b^{12}y^6 - \\ & 48b^{10}x^6y^2 - 204b^{10}x^4y^4 - 276b^{10}x^2y^6 - 120b^{10}y^8 - 24b^8x^{10} - 204b^8x^8y^2 - \\ & 612b^8x^6y^4 - 852b^8x^4y^6 - 564b^8x^2y^8 - 144b^8y^{10} - 36b^6x^{12} - 252b^6x^{10}y^2 - 720b^6x^8y^4 - \\ & 1080b^6x^6y^6 - 900b^6x^4y^8 - 396b^6x^2y^{10} - 72b^6y^{12} - 12b^4x^{14} - 84b^4x^{12}y^2 - 252b^4x^{10}y^4 - \\ & 420b^4x^8y^6 - 420b^4x^6y^8 - 252b^4x^4y^{10} - 84b^4x^2y^{12} - 12b^4y^{14} - 8b^{12}y^4 + 32b^{10}x^4y^2 + \end{aligned}$$

$$\begin{aligned}
 &126 b^{10} x^2 y^4 + 102 b^{10} y^6 + 40 b^8 x^8 + 332 b^8 x^6 y^2 + 826 b^8 x^4 y^4 + 816 b^8 x^2 y^6 + 282 b^8 y^8 + \\
 &110 b^6 x^{10} + 666 b^6 x^8 y^2 + 1564 b^6 x^6 y^4 + 1796 b^6 x^4 y^6 + 1014 b^6 x^2 y^8 + 226 b^6 y^{10} + \\
 &54 b^4 x^{12} + 324 b^4 x^{10} y^2 + 810 b^4 x^8 y^4 + 1080 b^4 x^6 y^6 + 810 b^4 x^4 y^8 + 324 b^4 x^2 y^{10} + \\
 &54 b^4 y^{12} - 4 b^{10} x^2 y^2 + 56 b^{10} y^4 - 36 b^8 x^6 - 164 b^8 x^4 y^2 - 228 b^8 x^2 y^4 - 92 b^8 y^6 - \\
 &148 b^6 x^8 - 716 b^6 x^6 y^2 - 1244 b^6 x^4 y^4 - 932 b^6 x^2 y^6 - 256 b^6 y^8 - 116 b^4 x^{10} - 572 b^4 x^8 y^2 - \\
 &1128 b^4 x^6 y^4 - 1112 b^4 x^4 y^6 - 548 b^4 x^2 y^8 - 108 b^4 y^{10} + 4 b^{10} y^2 + 17 b^8 x^4 + 14 b^8 x^2 y^2 - \\
 &143 b^8 y^4 + 126 b^6 x^6 + 294 b^6 x^4 y^2 + 136 b^6 x^2 y^4 - 36 b^6 y^6 + 141 b^4 x^8 + 492 b^4 x^6 y^2 + \\
 &622 b^4 x^4 y^4 + 332 b^4 x^2 y^6 + 61 b^4 y^8 + 2 b^2 x^{10} + 6 b^2 x^8 y^2 + 4 b^2 x^6 y^4 - 4 b^2 x^4 y^6 - \\
 &6 b^2 x^2 y^8 - 2 b^2 y^{10} - 4 b^8 x^2 - 20 b^8 y^2 - 60 b^6 x^4 - 20 b^6 x^2 y^2 + 172 b^6 y^4 - 132 b^4 x^6 - \\
 &200 b^4 x^4 y^2 + 28 b^4 x^2 y^4 + 96 b^4 y^6 - 16 b^2 x^8 - 32 b^2 x^6 y^2 + 32 b^2 x^4 y^4 + 16 b^2 y^8 + \\
 &16 b^6 x^2 + 40 b^6 y^2 + 70 b^4 x^4 + 16 b^4 x^2 y^2 - 98 b^4 y^4 + 38 b^2 x^6 + 38 b^2 x^4 y^2 - 38 b^2 x^2 y^4 - \\
 &38 b^2 y^6 - 24 b^4 x^2 - 40 b^4 y^2 - 28 b^2 x^4 - 8 b^2 x^2 y^2 + 20 b^2 y^4 + 16 b^2 x^2 + 20 b^2 y^2 + \\
 &x^4 + 2 y^2 x^2 + y^4 - 4 x^2 - 4 y^2 = 0
 \end{aligned}$$

Figure 3 shows the plot of these boundary curves for three cases. In the second and third cases, they divide the workspace into three regions. In the largest one, the manipulator admits two inverse kinematic solutions. In the two smaller regions (filled in grey), there are four solutions. Figure 4 shows the four inverse kinematic solutions for the manipulator defined by $L = 1$ and $b = 9/10$, at $x = 0$, $y = 1$.

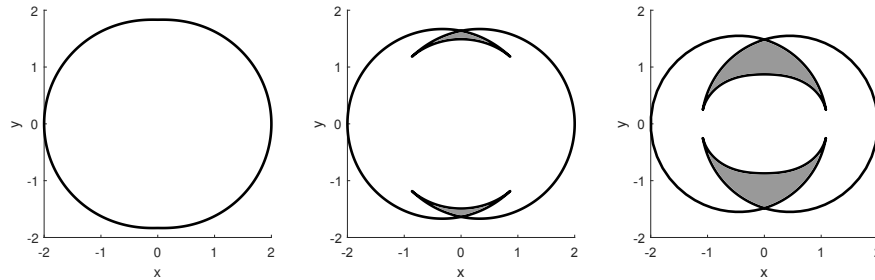


Fig. 3: Workspace boundaries when $L = 1$ and $b = 2/5$ (left), $b = 2/3$ (center), $b = 9/10$ (right)

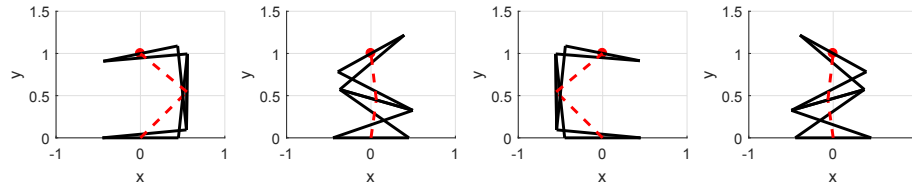


Fig. 4: The four inverse solutions at $x = 0$ and $y = 1$ ($L = 1$ and $b = 9/10$)

4 Conclusion

The equation of the boundary curves of the workspace of a 2-X manipulator was derived using the discriminant of the characteristic polynomial derived for the inverse kinematics. The resulting polynomial is of degree 16 and, under some geometric conditions, reveals regions with four inverse kinematic solutions. Moreover, the boundary curves of the 4-solution regions feature two cusp points and one node.

Acknowledgement This work has been conducted in part with the support of the French National Research Agency (AVINECK Project ANR-16-CE33-0025).

References

1. K. Moored et al., Analytical predictions, optimization, and design of a tensegrity-based artificial pectoral fin, *Int. J. of Solids and Structures*, Vol. 48, pp3142-3159, 2011
2. K. Snelson, Continuous Tension, Discontinuous Compression Structures, US Patent No. 3,169,611, 1965
3. D. L Bakker et al., Design of an environmentally interactive continuum manipulator, *Proc.14th World Congress in Mechanism and Machine Science, IFToMM'2015*, Taipei, Taiwan, 2015
4. R. B. Fuller, Tensile-integrity structures, United States Patent 3063521,1962
5. Skelton, R. and de Oliveira, M., *Tensegrity Systems*. Springer, 2009
6. S. Levin, The tensegrity-truss as a model for spinal mechanics: biotensegrity, *J. of Mechanics in Medicine and Biology*, Vol. 2(3), 2002
7. M. Arsenault and C. M. Gosselin, Kinematic, static and dynamic analysis of a planar 2-dof tensegrity mechanism, *Mech. and Mach. Theory*, Vol. 41(9), 1072-1089, 2006
8. C. Crane et al., Kinematic analysis of a planar tensegrity mechanism with prestressed springs, in *Advances in Robot Kinematics: analysis and design*, pp 419-427, J. Lenarcic and P. Wenger (Eds), Springer (2008)
9. P. Wenger and D. Chablat, Kinetostatic Analysis and Solution Classification of a Planar Tensegrity Mechanism, *proc. 7th. Int. Workshop on Comp. Kinematics*, Springer, ISBN 978-3-319-60867-9, pp422-431, 2017.
10. M. Furet et al., Kinematic analysis of planar 2-X tensegrity manipulators, *Proc. Advances in Robot Kinematics*, Bologna, Italy, June 2018.
11. M. Furet and P. Wenger, Workspace and cuspidality analysis of a 2-X planar manipulator, *Proc. 4th IFToMM Symposium on Mechanism Design for Robotics*, Udine, Italie, 2018.
12. Q. Boehler et al., Definition and computation of tensegrity mechanism workspace, *ASME J. of Mechanisms and Robotics*, Vol 7(4), 2015
13. JB Aldrich and RE Skelton, Time-energy optimal control of hyper-actuated mechanical systems with geometric path constraints, in *44th IEEE Conference on Decision and Control*, pp 8246-8253, 2005
14. S. Chen and M. Arsenault, Analytical Computation of the Actuator and Cartesian Workspace Boundaries for a Planar 2-Degree-of-Freedom Translational Tensegrity Mechanism, *Journal of Mech. and Rob.*, Vol. 4, 2012
15. J. El Omri and P. Wenger, How to recognize simply a non-singular posture changing manipulator, *Proc. 7th Int. Conf. on Advanced Robotics*, 215-222, 1995

16. P. Wenger, Cuspidal and noncuspidal robot manipulators. Special issue of *Robotica on Geometry in Robotics and Sensing*, Volume 25(6), pp.677-690, 2007
17. F. Thomas and P. Wenger, , On the Topological Characterization of Robot Singularity Loci. A Catastrophe-Theoretic Approach, IEEE International Conference on Robotics and Automation ICRA 2011, 9-13 mai 2011, Shanghai.
18. P. Wenger, D. Chablat, M. Baili, A DH parameter based condition for 3R orthogonal manipulators to have four distinct inverse kinematic solutions, *ASME Journal of Mechanical design*, Vol. 127(1), pp 150-155, 2005